SAND2018-2817C

Radar Doppler processing with nonuniform PRF

A. W. Doerry*

Sandia National Laboratories, P.O. Box 5800, MS 0519, Albuquerque, NM 87185

ABSTRACT

Conventional signal processing to estimate radar Doppler frequency often assumes uniform pulse/sample spacing. This is typically more for the convenience of the processing. More recent performance enhancements in processor capability allow optimally processing nonuniform pulse/sample spacing, thereby overcoming some of the baggage that attends uniform sampling, such as Doppler ambiguity and SNR losses due to sidelobe control measures.

Keywords: radar; PRF; Doppler; nonuniform

1 INTRODUCTION

The realm of pulse-Doppler radar systems is defined by the action of a sequence of pulses being transmitted, with echoes therefrom recorded and processed. Conventional processing across pulses especially in coherent systems often assumes the pulses are equally spaced, either in time or in spatial offset.

Uniform sample spacing is particularly convenient for conventional processing schemes that often employ efficient transforms such as the Fast Fourier Transform (FFT) for Doppler frequency calculations. Even when the collected data is not precisely uniform, data samples are typically resampled to a uniform spacing for subsequent processing. For data that are uniformly sampled, or even nearly so, a problematic consequence is the manifestation of grating lobes in their spectrum, leading to ambiguous Doppler frequency measures. We emphasize the point that strong Doppler grating lobes are a direct consequence of uniform sample spacing. In addition, another consequence to any Doppler frequency notches, such as for stationary clutter suppression, is that they too are repeated to form periodic "blind" velocities. Furthermore, a Doppler spectral analysis of uniform samples often requires amplitude tapering to control deleterious sidelobe responses, with the problematic side-effect of reducing Signal-to-Noise Ratio (SNR).

The conventional approach to resolving Doppler ambiguities is to stagger the Pulse Repetition Frequency (PRF) of the radar, with conventional uniformly spaced samples within the staggered subintervals, if the stagger interval is greater than a single pulse. Skolnik[1,2] provides an introduction to designing staggered PRF systems. Extended discussions can also be found in texts by Galati,[3] and by Schleher.[4] Applying a random "jitter" to the radar PRF has also been investigated, and is discussed by among others Vergara-Dominguez.[5] We note that early investigations often dealt with effects of suboptimal processing of such jittered PRF data. More recently, techniques have been explored to disambiguate Doppler in GMTI modes by examining residual range migration. Representative publications include those by Xia, et al.,[6] Zhu and Liao,[7,8] and Huang, et al.[9] The processing of sampled-data is also very related to array-antenna design and operation, with much of the mathematics readily transferable. More abstract treatments of non-uniform sampling are also available in a number of publications, including texts by Marvasti,[10] Yen,[11] Davis and Lanterman,[12] and Aldroubi and Gröchenig.[13]

We examine herein a more unconstrained sample spacing to facilitate advantage to unambiguously identifying Doppler spectral content. We note that Legg, et al.,[14] examined using a randomly varying PRF to disambiguate Doppler in a SAR image. Herein we extend these ideas to achieve further-improved performance. This paper is an abridged rendering of a more comprehensive report by the author.[15]

* awdoerr@sandia.gov; phone 505-845-8165; www.sandia.gov/radar

2 DETAILED DISCUSSION

2.1 Some Basics

To set up the following discussion, we begin by defining a generic signal $x(t)$ = continuous function of time *t*. As we will be interested in the Fourier Transform of functions, we accordingly define

$$X(f) = \int_{-\infty}^{\infty} x(t) e^{-j2\pi ft} dt \quad = \text{forward transform, and } x(t) = \int_{-\infty}^{\infty} X(f) e^{j2\pi ft} df \quad = \text{inverse transform,} \tag{1}$$

where the Fourier Transform is in terms of frequency *f*. We may use shorthand to identify the transform pair as

$$x(t) \Leftrightarrow X(f). \tag{2}$$

2.2 Periodic (Uniform) Sampling

We now define the periodic sampling function in the conventional manner and identify its transform, namely

$$\sum_n \delta(t - T_s n) \Leftrightarrow f_s \sum_u \delta(f - f_s u), \tag{3}$$

Where *n* = pulse index, *u* = spectral Nyquist band index, T_s = uniform sampling interval, $f_s = 1/T_s$ = constant sampling frequency, and $\delta(z)$ = Dirac delta function. The individual samples of $x(t)$ are then given (modelled) by

$$x_s(T_s n) = x(t)\delta(t - T_s n) = x(T_s n)\delta(t - T_s n), \tag{4}$$

and the sampled function is identified as

$$x_s(t) = \sum_n x(T_s n)\delta(t - T_s n). \tag{5}$$

We will generally assume that we have *N* samples of the function over an interval of duration *T*. For uniform periodic samples, we have $T = T_s N$. The Fourier Transform of the sampled function is well-known and given by

$$X_s(f) = X(f) * f_s \sum_u \delta(f - f_s u) = f_s \sum_u X(f - f_s u), \tag{6}$$

where "*" denotes convolution. The Fourier Transform can be expanded to

$$X_s(f) = \sum_n x(T_s n) e^{-j2\pi f T_s n}. \tag{7}$$

This is in fact the Discrete-Time Fourier Transform (DTFT). If we select uniformly spaced sample frequencies, where $f = (k/K) f_s$, where *K* = number of frequency samples over the interval $[0, f_s)$, then we may write

$$X_s\left(\frac{k}{K} f_s\right) = \sum_n x(T_s n) e^{-j2\pi \frac{k}{K} n}. \tag{8}$$

This is customarily referred to as simply the Discrete Fourier Transform (DFT) of the sequence $x(T_s n)$. We further note that the DFT is related to the continuous-time spectrum via Eq. (6), such that

$$\sum_u X\left(\frac{k}{K} f_s - f_s u\right) = T_s \sum_n x(T_s n) e^{-j2\pi \frac{k}{K} n} \ . \tag{9}$$

If $x(t)$ is suitably band-limited, then we may identify the baseband spectrum as specifically the case for $u = 0$, for suitable values of *k*. What is important to note here is that the calculation of the actual spectrum requires scaling the DFT result by the sampling interval T_s. This is typically 'not' what most implementations of the DFT, such as the Fast Fourier Transform (FFT), in fact calculate.

The Data Interval

We stipulate that we will generally be interested in a finite number of samples over a finite data collection interval. Accordingly, we identify our data characteristics for subsequent analysis as N = number of data samples, with $0 \le n \le N-1$, and T = data collection interval, with individual sample times $0 \le t_n < T$. These definitions will hold true for the remainder of this paper. Nevertheless, for periodic/uniform sampling, we identify $T_s = T/N$. With malice aforethought, we may also now write the baseband spectrum as

$$X(f) = \frac{T}{N} \sum_n x(t_n) e^{-j2\pi f t_n} \ . \tag{10}$$

2.3 Aperiodic (Nonuniform) Sampling

Let us now choose arbitrary sampling times such that our sampled function is

$$x_s(t) = \sum_n x(t_n) \delta(t - t_n) \, . \tag{11}$$

We will still generally assume that we have *N* samples of the function over an interval of duration *T*, but the samples at times t_n are no longer required to be uniformly spaced. The spectrum of this sampled function is then

$$X_s(f) = \int_{-\infty}^{\infty} \sum_n x(t_n) \delta(t - t_n) e^{-j2\pi ft} dt = \sum_n x(t_n) e^{-j2\pi f t_n} \ . \tag{12}$$

However, what we really want is an estimate of the continuous-time spectrum $X(f)$. This requires scaling the input signal samples according to their density, which we identify with a "local" sampling frequency and associated "local" sampling period as

$$\begin{aligned} &f_s(t_n) \text{ = local sampling frequency, and} \\ &T_s(t_n) = \left[f_s(t_n) \right]^{-1} \text{ = local sampling period (interval).} \end{aligned} \tag{13}$$

Note that these are now non-constant functions of t_n. Accordingly, our estimate of a band-limited continuous-time spectrum is identified as

$$X(f) = \sum_n T_s(t_n) x(t_n) e^{-j2\pi f t_n} \ . \tag{14}$$

We may still choose to index our spectral index to sampled frequencies where $f = (k/K) f_{ref}$, where now K = number of frequency samples over the interval $[0, f_{ref})$, with f_{ref} = a specified reference frequency. Since sampling is no longer periodic, we also no longer have the replicated spectra that Eq. (3) would otherwise imply. This means that the

aliasing that occurs with uniformly sampled data is subverted, allowing us to discriminate tonal signals beyond what otherwise might be a sampling bandwidth. We also stipulate that there is no particular reason other than convenience for sampled frequencies to be regular in the frequency domain. We will nevertheless to choose to do so hereafter anyway.

Local Sampling Frequency/Period Calculation

We now explore the relationship between sample times and the local sampling frequency/period calculations. Let us begin by defining a reference continuous function for the basis of sampling period calculations as

$$g(z) \text{ = some specific differentiable reference function.} \tag{15}$$

Here, the argument z is merely an arbitrary placeholder for now. We further identify that at specific integer arguments

$$g(n) = t_n . \tag{16}$$

Essentially, t_n are merely samples of $g(z)$ at integer arguments. Some additional properties include $g(0) = 0$, and $g(N) = T$. This allows us to identify the local sampling period as

$$T_s(t_n) = \frac{d}{dz} g(z)\bigg|_{z=n} = g'(z)\big|_{z=n} . \tag{17}$$

Otherwise, given the local sampling period, we may identify the sample positions as a summation of previous sampling periods, as we might expect, as

$$t_n \approx \sum_{m=0}^{n-1} T_s(t_m) . \tag{18}$$

This is only approximate due to the vagaries inherent in sample-time increments not being precisely equal to the local sampling period at a particular sample time. This difference diminishes for smooth functions as the number of sample times increases. Often, we will choose a $g'(z)$, but such that

$$\int_{z=0}^{N} g'(z) dz = T , \tag{19}$$

and therefrom calculate $g(z)$. Occasionally, however, we may in fact begin with $g(z)$ and therefrom identify $g'(z)$. Sometimes, iteration between the two might even be required. In any case, once we have a $g(z)$ and $g'(z)$ pair, we may use Eq. (16) and Eq. (17) to identify both sample times and local sampling period, as desired. We note that our choice of N samples in T seconds remains consistent with the case of uniform sampling. That is, we are not seeking advantage by increasing either of these over the uniform sampling case, but are merely rearranging the specific sample times to no longer be uniform. We note that Marvasti[10] shows that as long as the "average" sampling rate is not diminished, then nonuniform sampling offers no loss in information compared to uniform samples for band-limited signals.

2.4 Aperiodic (Nonuniform) Sampling with Window Tapers

Window taper functions are used in processing data to control processing sidelobe characteristics. There are many windows from which to choose, with various trades in parameters and characteristics.[16] We offer to employ a window

taper function with all the usual characteristics, including being real, even, and non-zero over the interval $[-1/2, 1/2]$, with unit DC gain. An example of such a window taper function is the Hann (a.k.a. Hanning) window, stipulated to be

$$w(z) = \begin{cases} (1 + \cos(2\pi z)) & |z| \le 1/2 \\ 0 & else \end{cases}, \tag{20}$$

Employing such a window function modifies our estimate of the band-limited continuous-time spectrum to

$$X(f) = \sum_n w\left(\frac{t_n}{T} - \frac{1}{2}\right) T_s(t_n)\, x(t_n)\, e^{-j2\pi f t_n} \ . \tag{21}$$

Of course, we may continue to index this to sampled frequencies where, as before $f = (k/K)\, f_{ref}$. We observe that to estimate the band-limited continuous-time spectrum in Eq. (21), the specific data samples are weighted with two distinct factors. The first is the local sampling period, and the second is the actual taper function. These two factors combine for a net data weighting being their product $\left[w(t_n/T - 1/2) T_s(t_n) \right]$.

Consider the special case where $w(t_n/T - 1/2) T_s(t_n) = T/N$ for all t_n. In this case, the window taper function is effectively incorporated into the sample spacing. That is, we get sidelobe control by sample spacing rather than amplitude tapering.

2.5 Aperiodic Sample Times Selection

Given the analysis in the previous sections, we summarize with the following procedure for selecting the sample times.

1. Select one of the functions $g'(z)$ and $g(z)$ for a desired characteristic, and calculate the other.
2. From the functions $g'(z)$ and $g(z)$, calculate the sample times t_n and local sample spacing $T_s(t_n)$ at those times, using Eq. (16) and Eq. (17).

For subsequent spectral analysis of the sampled signal, we might add the following steps.

3. Choose a final net window taper function $w(z)$.
4. Calculate the signal spectrum using Eq. (21), perhaps at specific frequencies $f = (k/K)\, f_{ref}$.

3 SAMPLING STRATEGIES

We now examine several sampling strategies. In all subsequent cases, we expect common parameters for the following.

N = number of data samples, with $0 \le n \le N - 1$, and
T = data collection interval, with $0 \le t_n < T$. (22)

Note that the "average" sampling rate will be held constant. In particular, for the following examples, we will assume $N = 1024$, and $T = 0.25$ s. To illustrate signal processing fidelity, we will also assume a noise-free signal

$$x(t) = e^{j2\pi[0.25\, N/T]t} = \text{arbitrary test signal.} \tag{23}$$

Unless indicated otherwise, we will also assume employment of a Hann window taper function.

3.1 Constant Sample Spacing (Reference)

To provide reference for following aperiodic sampling strategies, we begin with the conventional uniform sampling, conducive to FFT processing, where

$$g'(z) = T/N \text{ = constant sample time increments, and}$$
$$g(z) = (T/N)z \text{ = linear increment in sample times.} \quad (24)$$

For this first sampling of our reference signal we choose a constant PRF; a constant sample time increment. This is the conventional sampling strategy. Furthermore, we will employ a Hann window taper function. Figure 1 shows the sample-time increment as a function of essentially sample index. Note that this is constant. Figure 2 shows the spectrum of the signal. Note that for a uniform sampling strategy, we have replicated spectra at integer offsets of the constant PRF; these offset intervals being multiples of N/T. These grating lobes are well-understood. Otherwise, the structure of the response is precisely what we expect for using a Hann window taper function. Figure 3 is a zoomed version of the mainlobe response.

3.2 Staggered/Stepped Sample Spacing

A not-uncommon practice to disambiguate Doppler frequency is to stagger the radar PRF. This involves dividing the overall observation interval into multiple subintervals, with each sub-interval operating at a unique PRF. The information from the subintervals are then combined or compared to ascertain the proper Doppler estimate. We exemplify this technique by dividing the *N* pulses into four groups, each with an equal-number of pulses, and with the sample time increments illustrated in Figure 4. While various schemes can be concocted for how the spectra from the individual subintervals are combined, we shall combine the data coherently for a single spectrum response.

As we might expect, and as shown in Figure 5, we still have a maximum response at the correct signal frequency, but the regular grating lobes previously exhibited in Figure 2 have now had their energy divided into lesser grating lobes corresponding to aliasing due to the individual PRFs of the subintervals. Furthermore, the lesser lobes are broader as well. We do note that while the lesser grating lobes are reduced, some are still quite strong. For this reason, a more typical operating procedure would be to coherently process each subinterval separately, rather than as one single data set. Separate detections for the various subintervals would be compared, passing only those that coincided. This amounts to a voting scheme, or non-coherent filtering of the subinterval results. Since coherent processing is only over a subinterval, there is an attendant SNR loss, especially for low-SNR signals.

As the number of subintervals increases, we would observe a corresponding increase in the number of lesser grating lobes, but the strength of the individual aliased components would themselves decrease. We note that the stagger need not be generally increasing, and can in fact be randomly ordered. Furthermore, the specific PRF of the subintervals also need not be regularly spaced, nor do the lengths of the subintervals need be equal in time or in number of pulses.

3.3 Log-Periodic Sample Spacing

We now examine a "log-periodic" sample spacing; a sample spacing where the sample time increments change with each pulse in an exponential manner, i.e. where the log of the sample spacing is periodic. Specifically, we construct

$$g'(z) = (T/N)\left[b\,e^{az}\right] \text{ = sample time increments, and}$$
$$g(z) = (T/N)(b/a)\left[e^{az} - 1\right] \text{ = sample times,} \quad (25)$$

where *b* = the initial minimum sample spacing, and *a* = the exponential growth rate of the sample time increments. Note that we require *a* be found to satisfy $g(N) = T$. Figure 7 illustrates the case of $g'(z)$ with $b = 1/2$, and $a = 0.001228$.

Figure 8 shows the spectrum of the input signal so sampled, with the additional sample scaling of a Hann window taper function. Figure 9 details the mainlobe response and near-in sidelobes. We note that despite nonuniform sampling,

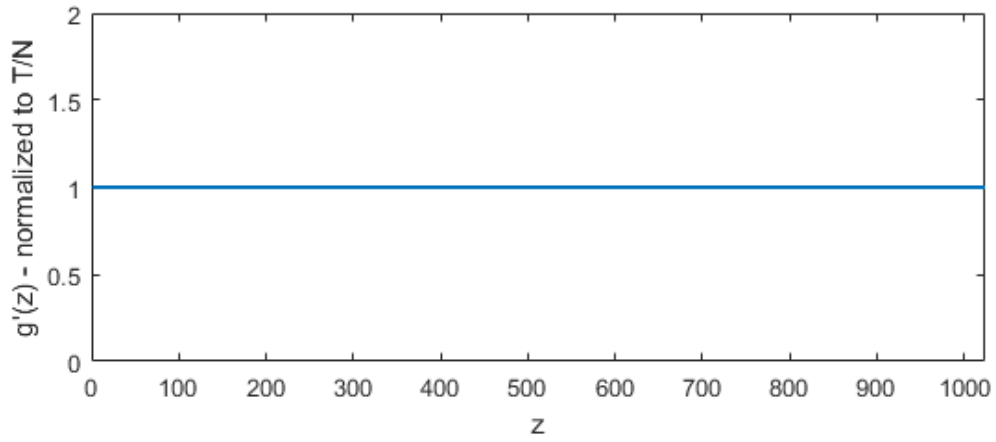

Figure 1. Sample-time increments normalized to *T/N*.

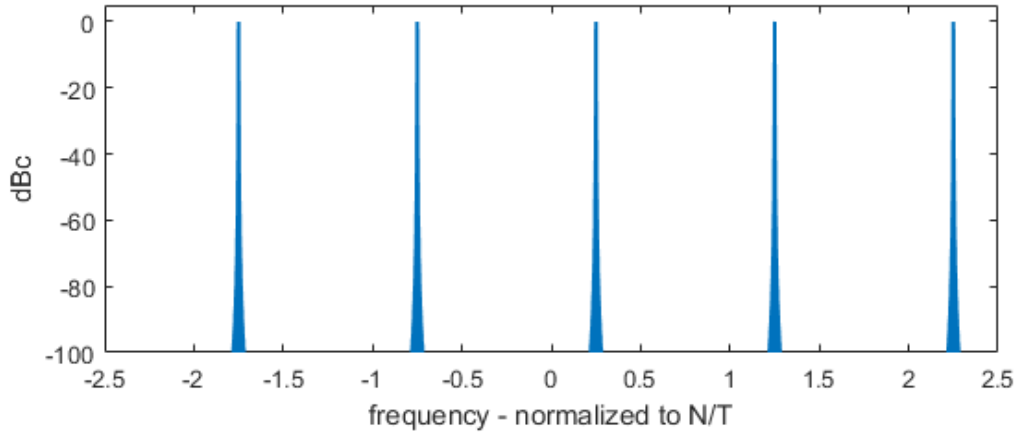

Figure 2. Spectrum of input signal with Uniform tapering.

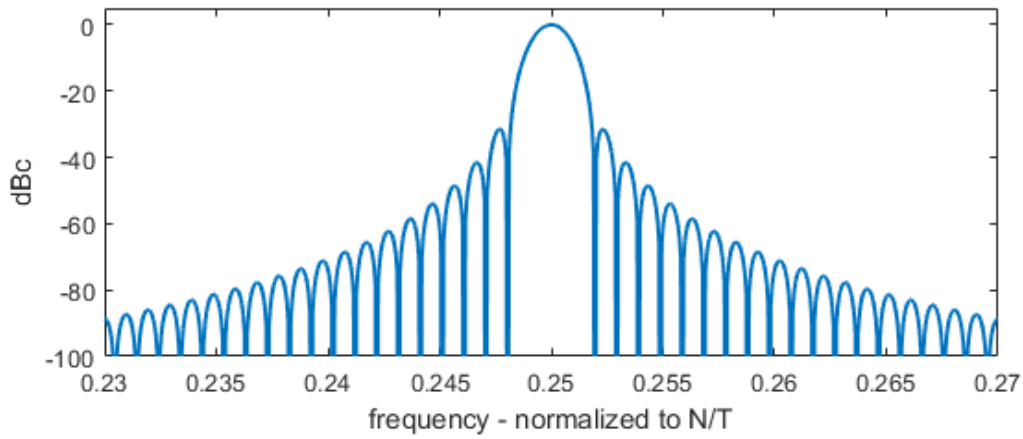

Figure 3. Zoomed rendering of Figure 2.

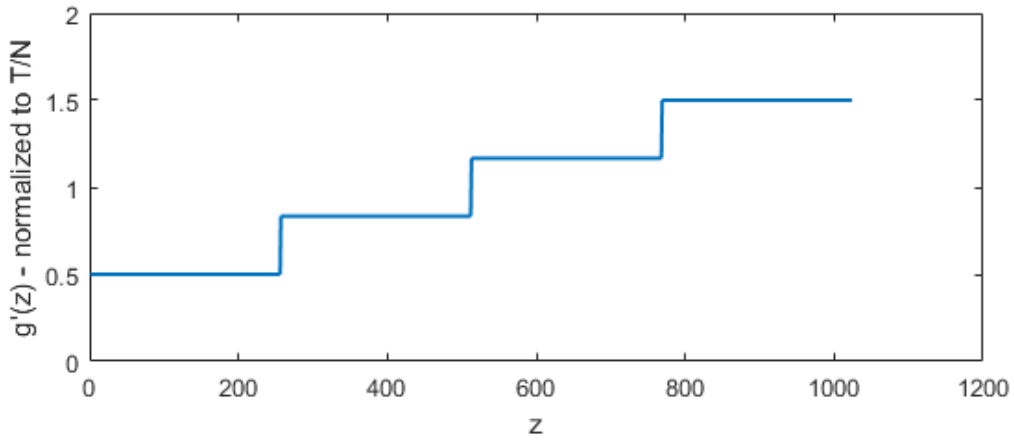

Figure 4. Sample-time increments normalized to *T/N*.

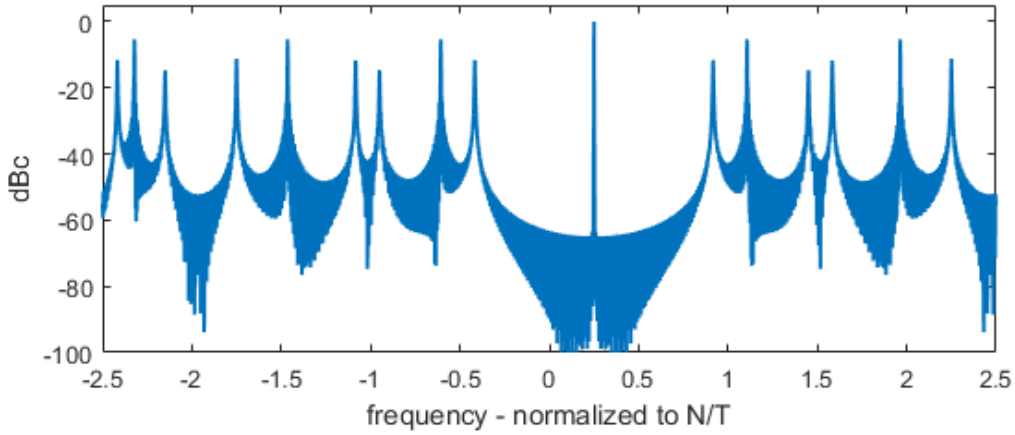

Figure 5. Spectrum of input signal using Hann window taper function.

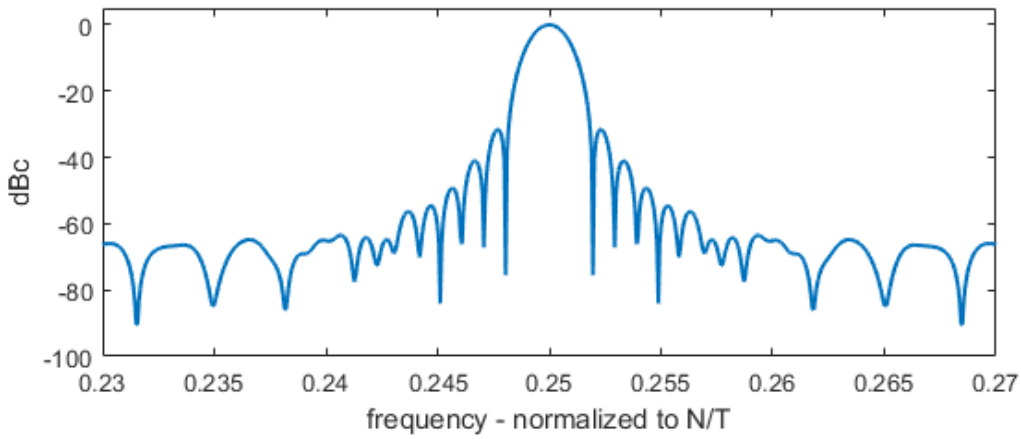

Figure 6. Zoomed rendering of Figure 5.

that the spectral response is virtually perfect for the mainlobe and a significant bandwidth around the mainlobe, in fact a region greater than N/T. We also note that the grating lobes evident in Figure 2 are absent, having been replaced by broadly smeared versions thereof with attendant reductions of at least 23 dB in this example. The reduction furthers as N increases. The coherence of any energy that otherwise might have been aliased in Doppler has been severely diminished. While we have shown here a log-periodic sampling, we stipulate that many other non-uniform sampling intervals will achieve similar results.

3.4 Discussion

One might ask whether uniformly sampled data can be resampled to nonuniform spacing and processed accordingly to advantage. Regrettably, this is not viable to remedy aliasing or Doppler ambiguity because the resampling process inherently assumes antialiasing filters built into the interpolation filter.[17] Consequently, since the aliasing is already "built in" to the data, it is not affected by subsequent processing, including interpolation.

It takes little imagination to construct other functions, some which might offer specific attributes desirable for some particular application. Important parameters for radar applications will be that $g'(z)$ and $g(z)$ conform to the characteristics discussed in section 2.3, with perhaps the additional constraint that $g'(z)$ be always greater than some minimum value determined by range-ambiguity requirements.

3.5 Spectrum Disambiguation

The real power of nonuniform sampling may be exemplified by examining the case of a signal with multiple frequencies. Accordingly, we put forth an example with the sum of three equal-amplitude tones with the following frequencies.

frequency #1 = $0.25\,N/T$,
frequency #2 = $-0.8\,N/T$, and
frequency #3 = $1.6\,N/T$.

Figure 10 illustrates the spectrum using Hann weighting with uniform sample spacing. Note that characteristic aliasing renders problematic ambiguity of the spectrum. Figure 11 illustrates the spectrum using Hann weighting but with log-periodic sample spacing as described in Figure 7. We note that what otherwise would have been aliased signals have been smeared to render essentially background noise, thereby clearly revealing the true disambiguated spectral components. Figure 12 illustrates the same calculations as Figure 11, except that 16 times the number of signal data samples were used, but with constant ratio N/T, implying T was extended by the same factor. Note the background smearing is to a significantly lower level.

4 CONCLUSIONS

Uniform sample spacing, while particularly "nice" to process, nevertheless exhibits the well-known baggage of aliasing due to grating lobes leading to ambiguous spectrum measurements. Adjusting sample times to nonuniform spacing interferes with aliasing, and can disambiguate spectral calculations. The nonuniform nature of useful sampling strategies might be deterministic, random, or chaotic. Proper spectrum calculations must consider not only the actual nonuniform sample times, but also the local sample spacing at those times. Window taper functions for sidelobe control must also be adjusted to actual sample times.

For radar Doppler analysis, conventional transform-based frequency estimation such as the FFT are inadequate to the task for processing nonuniform-spaced samples. However, the more recent viability of back-projection processing techniques also makes viable the more general calculations necessary for samples with nonuniform spacing. Employing smooth variations in sample spacing often allows a cleaner spectrum. This suggests that a smooth deterministic sample-spacing modulation is preferable to one with random steps or jumps. This analysis is readily extensible to other sampling applications.

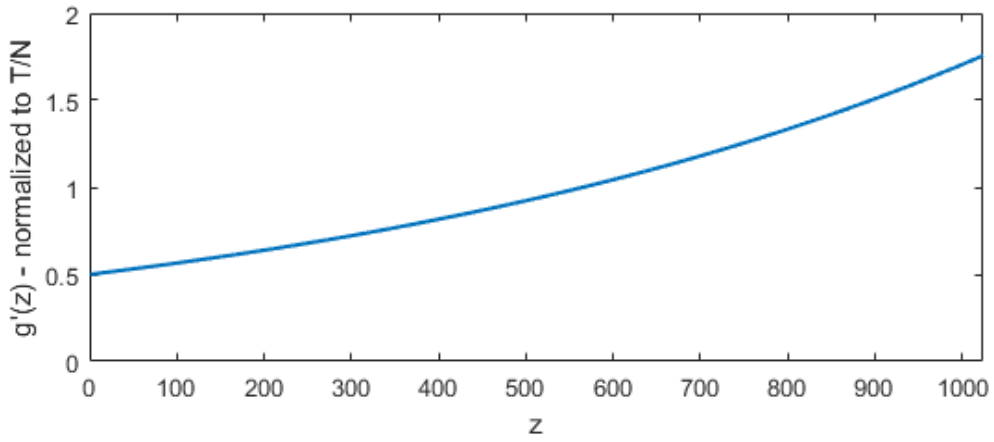

Figure 7. Sample-time increments normalized to *T/N*.

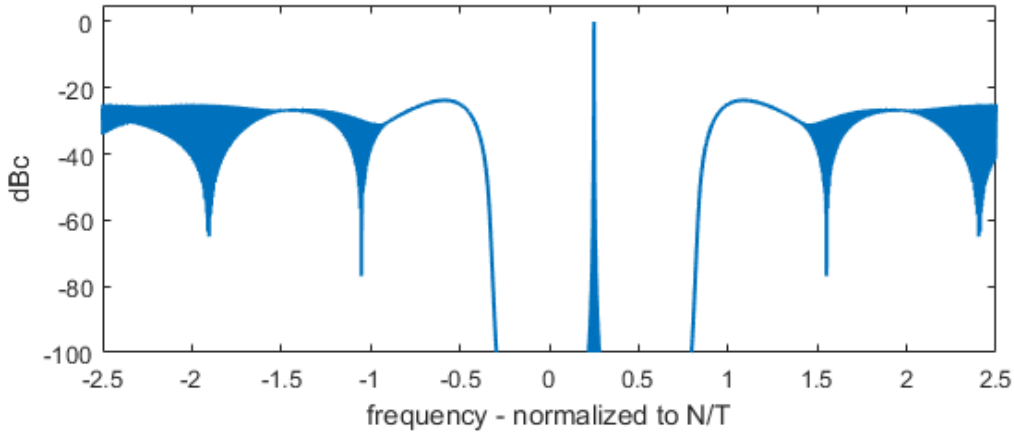

Figure 8. Spectrum of input signal using Hann window taper function.

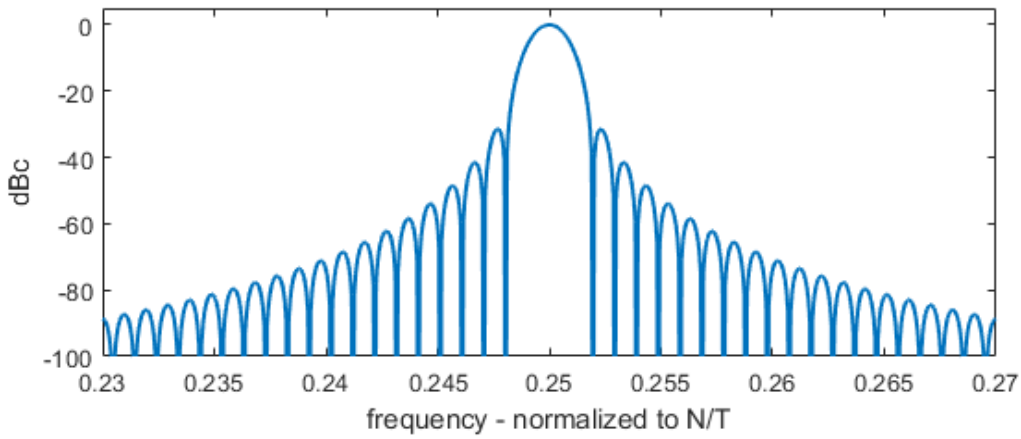

Figure 9. Zoomed rendering of Figure 8.

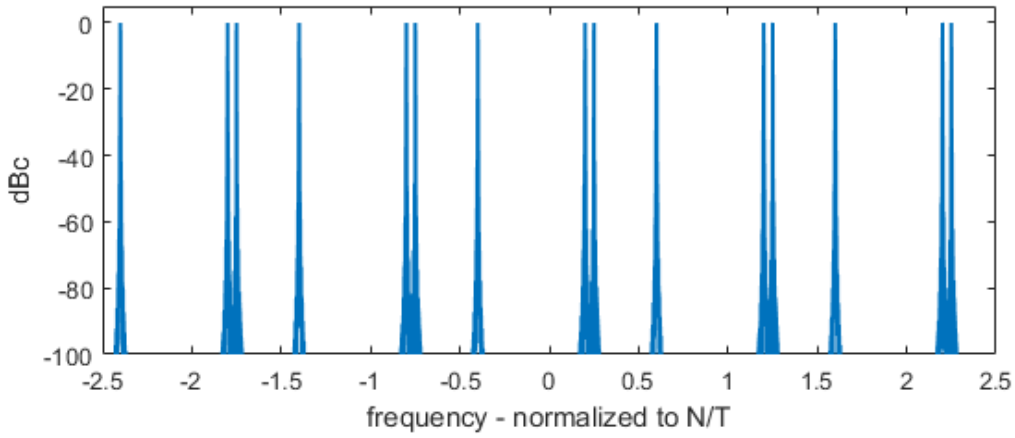

Figure 10. Spectrum of input signal using Hann window taper function, and uniform sample spacing.

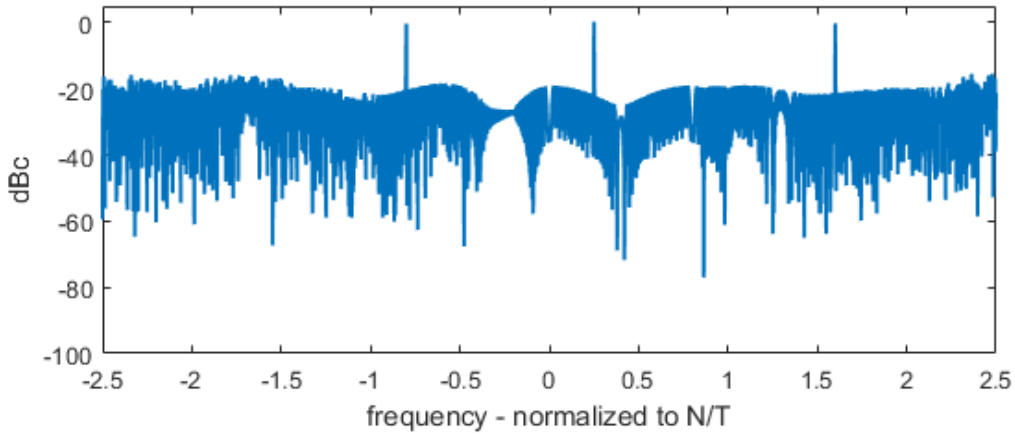

Figure 11. Spectrum of input signal using Hann window taper function, and log-periodic sample spacing.

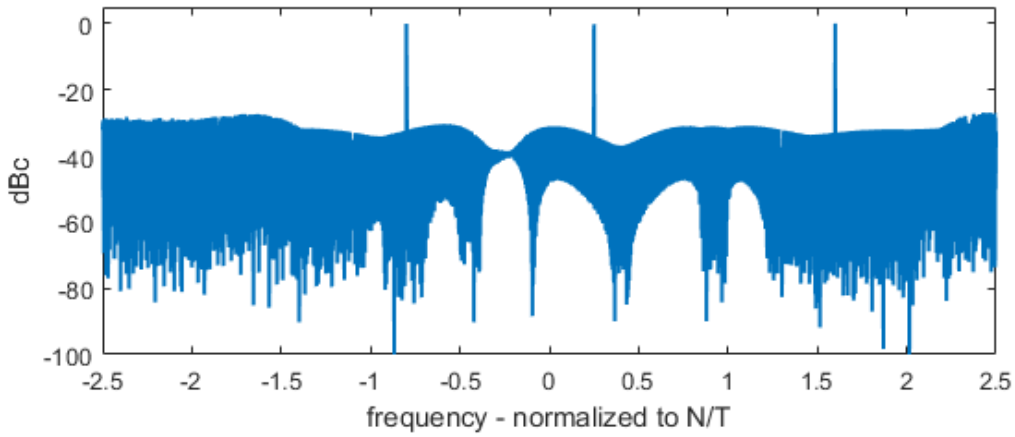

Figure 12. Same as Figure 11, except with 16 times the number of signal data samples.

ACKNOWLEDGEMENTS

Sandia National Laboratories is a multimission laboratory managed and operated by National Technology and Engineering Solutions of Sandia, LLC., a wholly owned subsidiary of Honeywell International, Inc., for the U.S. Department of Energy's National Nuclear Security Administration under contract DE-NA-0003525.

REFERENCES

[1] Merrill I. Skolnik, *Introduction to Radar Systems – second edition*, ISBN 0-07-057909-1, McGraw-Hill, Inc., 1980.

[2] Merrill Skolnik (ed.), *Radar Handbook – third edition*, ISBN 978-0-07-148547-0, McGraw-Hill, Inc., 2008.

[3] Gaspare Galati, *Advanced Radar Techniques and Systems*, ISBN 0-86341-172-X, Peter Peregrinus Ltd., on behalf of Institute of Electrical Engineers, 1993.

[4] D. Curtis Schleher, *MTI and Pulsed Doppler Radar with Matlab – second edition*, ISBN-13: 978-1-59693-414-6, Artech House, Inc., 2010.

[5] L. Vergara-Dominguez, "Analysis of the digital MTI filter with random PRI," *IEE Proceedings-F*, Vol. 140, No. 2, pp. 129-137, April 1993.

[6] B. Xia, J. Xu, Y.-N. Peng, X.-G. Xia, J. Tang, "Doppler ambiguity resolving for SAR moving targets via linear migration correction," *Electronics Letters*, Vol. 47, No. 7, 31st March 2011.

[7] Shengqi Zhu, Guisheng Liao, "A New Unambiguous Radial Velocity Estimation Approach of Ground Moving Targets for SAR System," *Proceedings of the 2011 IEEE Radar Conference (RADAR)*, pp. 702-705, 2011.

[8] Shengqi Zhu, Guisheng Liao, "Estimating Ambiguity Number of Radial Velocity for Ground Moving Targets from a Single SAR Sensor," *Proceedings of the 2011 XXXth URSI General Assembly and Scientific Symposium*, pp. 1-4, 2011.

[9] Yan Huang, Guisheng Liao, Jingwei Xu, Jie Li, "GMTI and Parameter Estimation via Time-Doppler Chirp-Varying Approach for Single-Channel Airborne SAR System," *IEEE Transactions on Geoscience and Remote Sensing*, accepted for publication, 2017.

[10] Farokh Marvasti (ed.), *Nonuniform Sampling: Theory and Practice (Information Technology: Transmission, Processing and Storage)*, ISBN 0306464454, Springer, 2001.

[11] J. L. Yen, "On Nonuniform Sampling of Bandwidth-Limited Signals," *IRE Transactions on Circuit Theory*, pp. 251-257, December 1956.

[12] Michael S. Davis, Aaron D. Lanterman, "Aliasing in Recurrently Sampled Signals With an Application to Synthetic Aperture Imaging," *IEEE Transactions on Signal Processing*, Vol. 63, No. 12, pp. 3088-3095, June 15, 2015

[13] Akram Aldroubi, Karlheinz Gröchenig, "Nonuniform Sampling and Reconstruction in Shift-Invariant Spaces," *SIAM Review*, Vol. 43, No. 4, pp. 585–620, 2001.

[14] Jonathan A. Legg, Alan G. Bolton, Douglas A. Gray, "SAR moving target detection using non-uniform PRI," *Proceedings of EUSAR'96*, pp. 423-426, Königswinter, Germany, 1996.

[15] Armin W. Doerry, *Radar Doppler Processing with Nonuniform Sampling*, Sandia National Laboratories Report SAND2017-7851, Unlimited Release, July 2017.

[16] Armin W. Doerry, *Catalog of Window Taper Functions for Sidelobe Control*, Sandia National Laboratories report SAND2017-4042, Unlimited Release, April 2017.

[17] A. W. Doerry, E. Bishop, J. Miller, V. Horndt, D. Small, "Designing interpolation kernels for SAR data resampling," SPIE 2012 Defense, Security & Sensing Symposium, Radar Sensor Technology XVI, Vol. 8361, Baltimore MD, 23-27 April 2012.